FOCUSED ISSUE FEATURE

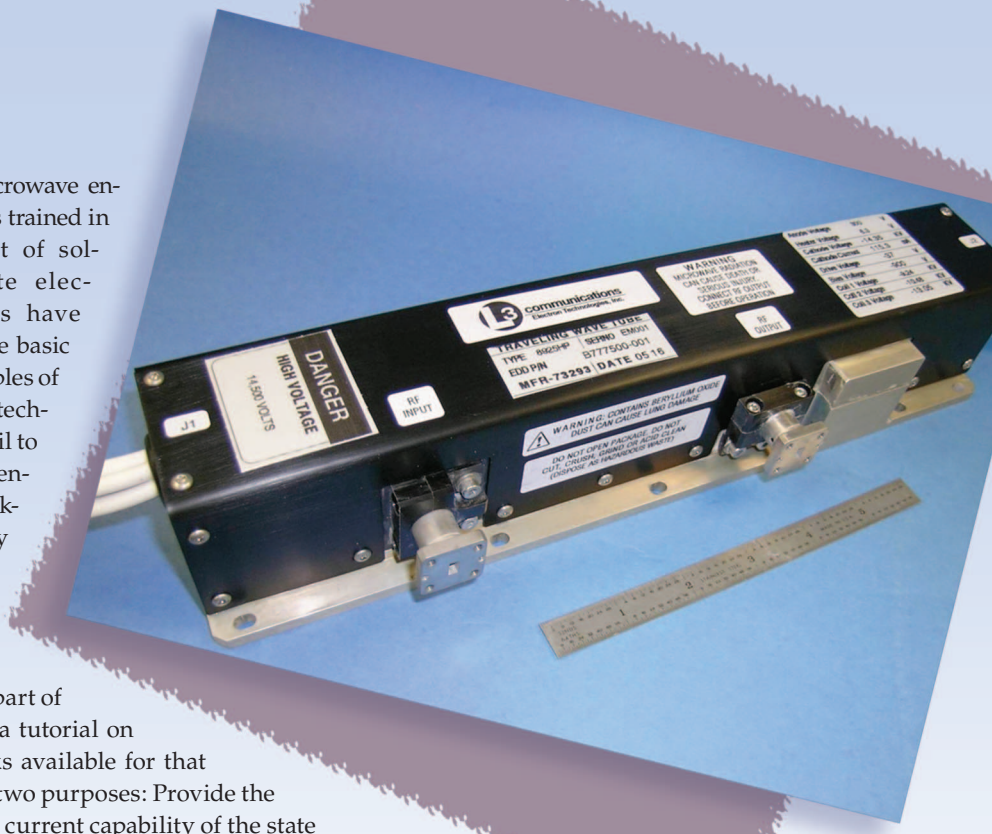

COURTESY OF L-3 ELECTRON TECHNOLOGIES, INC.

Most microwave engineers trained in the art of solid-state electronics have had little or no exposure to the basic physics and operational principles of modern vacuum electronics technology. Consequently, many fail to appreciate the capability, efficiency, and reliability of this remarkable and durable technology and fail to take advantage of it as a cost-effective, high-power solution when making system-level decisions. The goal of this article is to bridge part of this gap. It is not intended as a tutorial on the subject; there are textbooks available for that purpose [1], [2]. Instead, it has two purposes: Provide the reader with an overview of the current capability of the state of the art and provide a glimpse of the research trends of the near future. More information and in-depth analysis can be found in [3], which contains an excellent collection of review articles covering broad aspects of vacuum electronics science and technology.

Vacuum electronics technology is both old and new; its legacy is impressive and well-known. However, record

Vacuum Tube Amplifiers

Joe X. Qiu, Baruch Levush, John Pasour, Allen Katz, Carter M. Armstrong, David R. Whaley, Jack Tucek, Kenneth Kreischer, and David Gallagher

Joe X. Qiu (joe.qiu@arl.army.mil) is with the Army Research Laboratory, Adelphi, MD 20783. Baruch Levush and John Pasour are with the Naval Research Laboratory, Washington, DC 20375. Allen Katz is a professor in the Electrical and Computer Engineering Department at The College of New Jersey, and is President of Linearizer Technology, Inc., Hamilton, New Jersey 08619. Carter M. Armstrong and David R. Whaley are with Electron Devices Division, L-3 Communications, San Carlos, California 94070. Jack Tucek, Kenneth Kreischer, and David Gallagher are with Northrop Grumman Corporation, Rolling Meadows, Illinois 60008.

Digital Object Identifier 10.1109/MMM.2009.934517

 1527-3342/09/$26.00©2009 IEEE

levels of performance and reliability are now evolving via modern innovations that exploit new materials, electromagnetic structures, fabrication techniques, and designs. Vacuum electronics technology has been and will continue to be the enabling technology for entire classes of high-power, high-frequency amplifiers, with the most demanding specifications for use in both military and commercial systems. These demands are steadily driving designers of electronic systems into the frequency/power parameter space that is the natural domain of vacuum electronics technology. In addition to a wide variety of military and commercial applications requiring high power at high frequency, vacuum electronics (VE) amplifiers and oscillators are used in scientific research areas such as high-energy particle accelerators and plasma heating for controlled thermonuclear fusion. They are also widely used in many medical systems, such as compact radio-frequency (RF) accelerators and, recently, in nuclear magnetic resonance spectrometers for dynamic nuclear polarization experiments [4]. Commercial satellite communication systems, broadcasting, and microwave ovens for industrial and home use are also heavily dependent on vacuum devices for reliable performance at high power, high efficiency, and low cost. Only vacuum electronic devices meet many of these demanding requirements [5], [6]. Figure 1 shows the range of power and frequency for key applications.

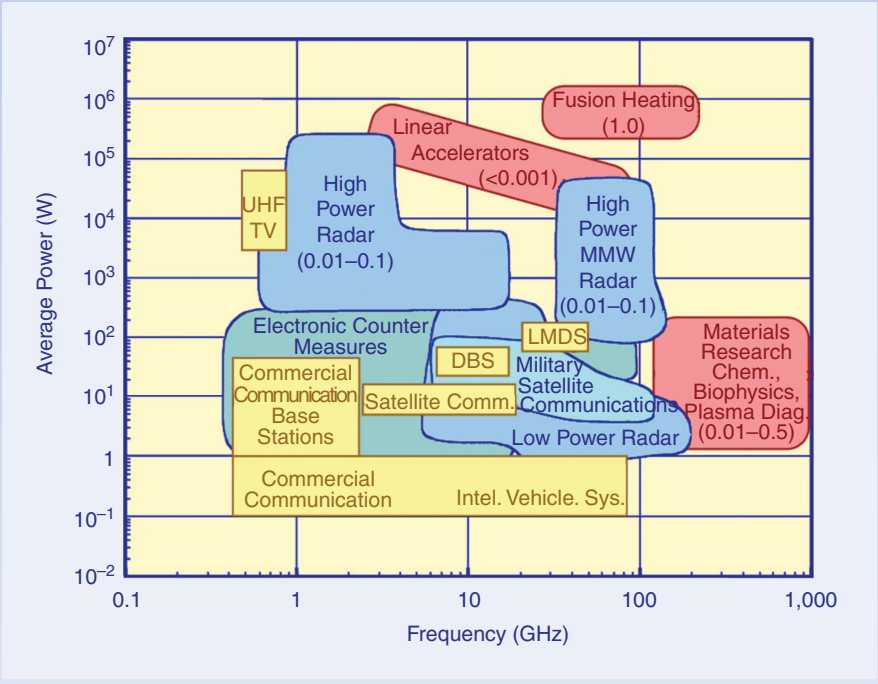

Figure 1. *Applications for high-power amplifiers in terms of average power versus frequency.*

The figure of merit, Pf^2, captures the ability of a device to generate RF power, where P is the average power and f is the operating frequency. Figure 2 shows the steady progress in Pf^2 achieved for various vacuum electronics device types. For example, Pf^2 for helix traveling-wave tubes (TWTs) has seen a three-order-of-magnitude improvement in the past 50 years and is poised for further growth with continued innovations, such as using brace support rods and CVD diamond support rods for more efficient heat removal [7].

Noteworthy improvements in vacuum electronics amplifier reliability have been realized over the past several decades. The operational lifetimes of the principal types of vacuum electronic amplifiers, always substantial, are now remarkable. For example, space-based applications require service lifetimes in excess of 150,000 hours (18 years); current data for space-based traveling-wave tube amplifiers (TWTAs) show a mean-time-to-failure of 8 million hours [8]. Such reliability improvements have led to significant reductions in operating cost for many systems.

In the meantime, solid-state power amplifiers (SSPAs) are also making great strides in improving their capability with ever increasing output power and higher operating frequency, and relentlessly invading the traditional performance realm of vacuum electronics technology [9] (Figure 3). These improvements are

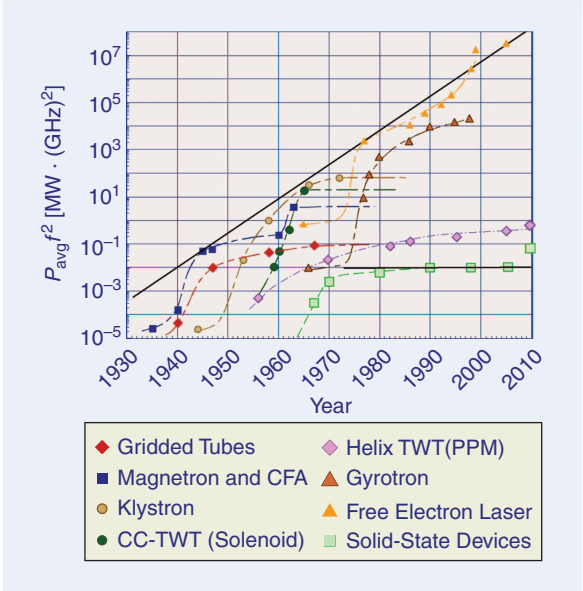

Figure 2. *Seven decades of progress in Pf^2 for various power amplifier types.*

Most microwave engineers fail to appreciate the capability, efficiency, and reliability of vacuum electronics technology.

made possible by the advances in devices based on wide bandgap semiconductor material (GaN), as well as more efficient power combining techniques [10], [11]. As a result, the power advantage of tube-based amplifiers over SSPAs is no longer obvious at lower microwave frequencies, although they still have better efficiency than SSPAs. In response to the challenges and market demand, the last decade has seen significant efforts by the VE industry to develop devices with higher power and greater bandwidth at the millimeter-wave band. More than 1 kW of millimeter-wave power can now be produced with high efficiency in a relatively small package [12].

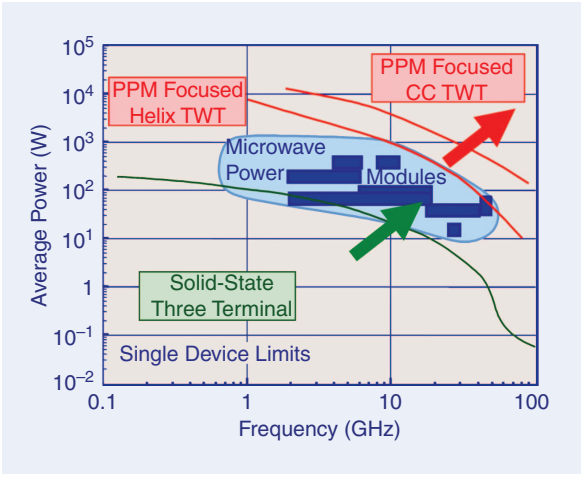

Figure 3. *Performance domain for the different high-power amplifier technologies: Traveling-wave tubes (TWTs) including helix and coupled-cavity types, microwave power modules (a solid-state and TWT hybrid) and solid-state power amplifiers. Also shown is the common development trend for the different technologies: higher power and higher frequency.*

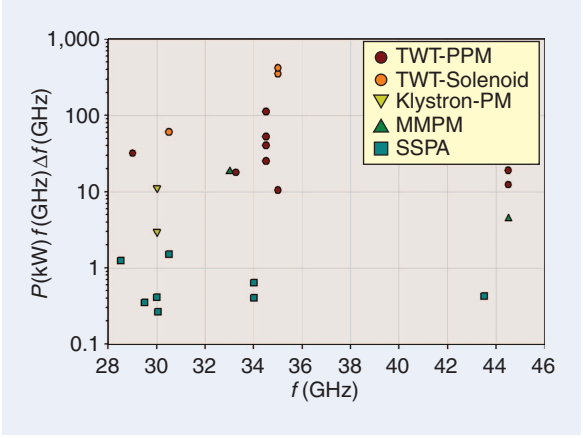

Figure 4. *The figure of merit $Pf^2(\Delta f/f)$ for selected millimeter-wave power amplifiers including traveling-wave tube (TWT) amplifier, millimeter-wave power module (MMPM), klystron, and solid-state power amplifier (SSPA).*

Common to both defense and commercial applications is the need for increased signal power to achieve the required signal-to-noise ratios over large transmission distances and large-signal bandwidth (which, in turn, calls for higher operating frequencies) to accommodate massive volumes of data. To measure the ability of the devices to transmit information, the figure of merit $Pf^2\,(\Delta f/f)$, where $(\Delta f/f)$ is the fractional instantaneous bandwidth of an amplifier, is plotted for a number of amplifiers at or above 30 GHz in Figure 4. The high mark of a 100 kW GHz^2 is achieved by a 35 GHz helix TWT with a periodic permanent magnet for beam focusing. Presently, about 1 kW GHz^2 is achieved by a 35 GHz SSPA. The larger value, about 500 kW GHz^2, for solenoid focusing devices is because of their ability to transmit more current than devices with periodic permanent magnet. However, solenoid magnets are bulky and heavy and require a separate power supply and cooling. As will be discussed later, the ongoing research effort to use a spatially distributed beam, such as a sheet beam, would enable the achievement of greater than 500 kW GHz^2 in a smaller permanent magnet.

Next, we will give a brief overview of the common tube amplifiers used in high-power transmitters. Only three types of devices [TWTs including helix and coupled-cavity types, microwave power modules (MPMs), and klystrons] will be covered, with emphasis on the recent advance in the millimeter-wave band. References to other tube devices can be found in the many proceedings of the IEEE International Vacuum Electronics Conference, as well as in the special issues on vacuum electronics of *IEEE Transactions on Electron Devices*. These publications contain a significant number of papers from countries such as Russia, China, France, Japan, South Korea, Italy, and the United Kingdom.

Current Status of TWTAs

In the design of high-power transmitters for airborne, space, and mobile applications, a strong emphasis is placed on minimizing the power consumption, applied voltage, size, and weight of the amplifiers. For such applications, where instantaneous bandwidth is also a requirement, helix and coupled-cavity TWTs are the device types of choice.

The main reasons for the continued reliance on vacuum electronic amplifiers such as TWTAs in space-based transponders and ground terminals are TWTAs' high output power and high efficiency. The typical available powers for commercial satellite communication TWTAs and SSPAs are compared in Figure 5. The power advantage of TWTAs over SSPAs is significant, especially at the higher frequency bands. At the lower frequency bands, on the other hand, the TWTAs'

grip on power is being challenged by SSPAs. For example, at C-band, commercially available modular SSPAs are capable of producing 1.5 kW of output power, and 3.0 kW by phase-combining two systems [13]. However, these SSPAs are still relatively inefficient, with efficiency at less than 20%. Compared to a linearized TWTA (LTWTA) producing similar RF power, the above SSPA would cost US$14,000 more in annual electricity cost [14].

Collector depression is a common technique for improving the efficiency of TWTs [1]. Using a depressed collector, one can convert some of the kinetic energy in the spent electron beam (i.e., after its interaction with the slow-wave circuit) into the potential energy of the power supplies and, therefore, increase the overall efficiency of the device [1, ch. 14]. Additional improvement can be achieved by employing a multistage depressed collector (MSDC) that can better match the energy distribution of the spent beam. The total efficiency of state-of-the-art space TWTs with a MSDC is over 70% [15] with typical TWTA efficiency between 50–60%. The typical SSPA's efficiency is about 25–30% [16].

The linearity of a power amplifier is always of great importance. For communication applications, the TWTA has long been considered as a device with poor linearity as compared to the SSPA. The general belief is that a TWTA must be backed off 3–4 dB from saturation to achieve the same level of linearity as an SSPA. This is an incomplete statement. It was pointed out in [16] that the power consumed by a TWTA is usually less than that of an SSPA with only half of the rated RF power. As a result, for two amplifiers with the same total power consumption, a TWTA generally has more available linear power than an SSPA for most of the frequency band. The two amplifiers have the same linearity performance for lower-power and lower-frequency amplifiers only. Furthermore, the linearity of a TWTA can be improved much more by use of linearization than that of an SSPA. As a result, more of the TWTA's RF power that is lost due to output backoff is available as linear power.

Predistortion linearization is a simple and effective technique for improving the performance of both SSPAs and TWTAs [17]. Its effectiveness on TWTAs is more significant because of the slow approach to saturation and the higher nonlinearity of the TWTA. It has been shown that by applying fifth-order linearization, it is possible to achieve less than 1 dB overall gain compression at saturation so that the combined transfer curve approaches that of an ideal linear limiter [18]. Consequently, the need for backoff from saturation can be greatly reduced to take advantage of the higher efficiency near saturation.

The effect of reduced efficiency by operating significantly below saturation to obtain linearity can be mitigated by reoptimizing the helix circuit for reduced gain compression and phase shift. It can also be mitigated by reoptimizing the MSDC (both the collector

Only vacuum electronic devices meet many of the demanding requirements for reliable performance.

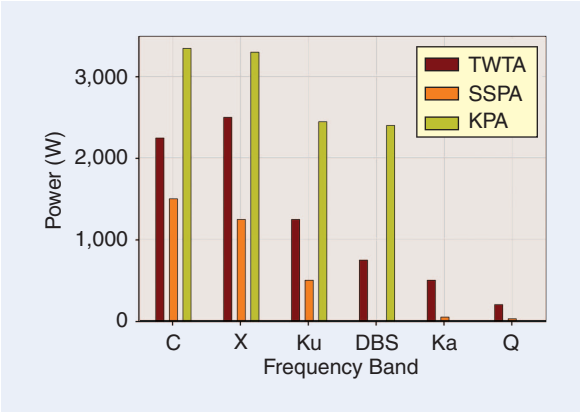

Figure 5. *Typical power of commercial satellite communication high-power amplifiers including traveling-wave tube amplifier (TWTA), klystron power amplifier (KPA) and solid-state power amplifier (SSPA).*

design and depressed voltages) to better match the spent beam distribution at large backoff operation. This will improve the collector efficiency and, therefore, the total efficiency. L-band and S-band TWTs at 200–300 W output with 25–40% efficiency and eight-tone carrier-to-intermodulation ratio levels of −70 dBc have been produced with this technique. This performance is a significant improvement over solid-state systems having the same fidelity and twice the efficiency of SSPA [19].

Recently, a new unexplored regime of TWT operation, based on the transverse interaction between an electron beam and a circularly polarized circuit was investigated [20]. It was predicted that a C-band transverse TWT could be more efficient and more linear—12 dB smaller value for the carrier-to-intermodulation ratio—than a conventional longitudinal TWT with a comparable saturated power. Such TWTAs, if implemented, could meet the demanding requirement for high-data-rate communication.

The last decade has also seen a leap in the performance of helix TWTs. These devices have critical applications in high-data-rate communications, high-resolution radar, and broadband electronic warfare. For example, in [21], a record helix TWT performance has recently been reported at C- and X-band, with 25 kW and 8 kW peak power for radar applications. Compact (around 3.5 lb) helix TWTs at Ka-band (30 GHz) with 500 W continuous wave (CW) power, and 55% efficiency and at Q-band (44 GHz), with 230 W CW power and 43% efficiency [22] have been demonstrated for communication applications. A major contributing factor for the millimeter-wave TWT

The power advantage of traveling-wave tubes over solid-state power amplifiers is significant, especially at the higher frequency bands.

achievements is the use of a simulation-based design methodology. This design methodology relies heavily on the suite of recently developed codes for vacuum electron devices [23]–[25].

A coupled-cavity TWT uses a slow-wave circuit that is mechanically and thermally more robust than a helix. A coupled-cavity structure is usually larger in size than a helix structure at the same frequency. It can, therefore, provide higher power at the same frequency or operate at much higher frequencies than a helix TWT. One example is Communication Power Industries, Inc.'s Millitron coupled-cavity TWT [26]. It is capable of producing 3 kW peak and 300 W average power at W-band.

Current Status of Microwave and Millimeter-Wave Power Modules

The MPM [27], [28] is an example of what Robert Symons calls *appropriate technology* [29]. In the case of a low noise, high efficiency compact microwave or millimeter-wave power amplifier, the appropriate technology to use is solid state for the input amplification and vacuum electronics for the output. This gain partitioning between solid state and vacuum electronics is what defines the MPM. When married with a miniaturized electronic power conditioner, a high-power-density RF amplifier module results, providing 100 W and higher in the microwave bands and 50 W and higher in the millimeter-wave bands. The combined performance in size, weight, efficiency, bandwidth, and noise level is unattainable using either constituent technology alone. Due to its small size and high efficiency, the MPM is particularly well-suited for use in resource-constrained applications, including communication (wireless), radar, and electronic warfare.

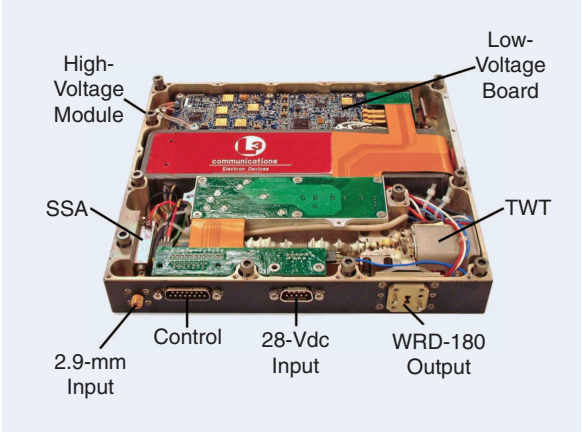

Figure 6. *40 W Ka-band microwave power module with components/subassemblies identified. SSA: solid state amplifier. TWT: traveling wave tube. Microwave power module cover has been removed.*

A millimeter-wave power module (MMPM), as the name suggests, is simply a MPM designed to operate in the millimeter-wave frequency bands. MMPMs have been developed at both Ka- and Q-band. A photograph of a first-generation Ka-band MMPM is shown in Figure 6. In the unit shown, a nominal 100 mW solid-state gallium arsenide (GaAs) amplifier drives a low-voltage (about 7 kV) compact vacuum power booster helix TWT. The MMPM provides an output power of 40 W from 26 to 40 GHz (with 50 W in the 30–31 GHz communication band) in a conduction-cooled package of 7.5 in × 8.5 in × 1.25 in, weighing 6 lbs. The module displayed operates from 28 V dc input power, requiring 300 W (max); however, other prime power formats, including 270 V dc and three-phase 115 V ac, are possible. All high voltage is self-contained within the module.

Since its initial development in the 1990s, the MPM has made significant strides in both performance and functionality. Second-generation Ka- and Q-band MMPMs currently under development at L-3 Communications Electron Devices provide twice the output power (100 W) at nearly double the efficiency (33%) over the first-generation designs. These advances are the result of the wholesale application of advanced modeling and simulation in component design [23], [24], as well as the steady progression in miniature multistage TWT collector technology and incremental improvements in power conditioning efficiency. Interestingly, although the power of the second-generation MPMs and MMPMs has doubled, their size and weight have not increased accordingly. The result is an increase in RF power density, 1.4 × power density (W/volume) and 1.6 × specific power density (W/mass), over first-generation performance.

The addition of a miniature predistortion linearizer [30] in the MPM RF chain results in an increase in rated linear power of two and one-half times (over operation without a linearizer) with a concomitant increase in rated efficiency by a factor of two. Such improvements in linear performance are important for digital and multicarrier communication applications.

Future directions in MPM and MMPM development point to the continued evolution of MPM performance and functionality. In the power-frequency realm, wideband dual-mode operation covering the Ka- and Q-communication bands in a single MPM with a single TWT is envisioned. While moving higher in frequency, compact W-band MPMs providing 100 W for radar and communication are seen as

enabling the exploitation of this region of the electromagnetic application space.

MPM functionality will also continue to increase. Most of this increase will come through higher levels of integration, such as that exhibited by the MPM transmitter (MPM-T). The MPM-T unit is a MPM assembly providing integral cooling, reverse and forward power sampling, linearization, harmonic and electromagnetic interference (EMI) filtering, serial interface control, and optional input signal up-conversion. The MPM-T, therefore, provides the system user a drop-in transmitter subassembly while still retaining all the desirable performance attributes of the MPM. A comparison of 75–100 W solid state and MPM forced air-cooled Ka-band amplifiers shows the MPM-T to be a factor of two times smaller, lighter, and more efficient than an equivalent SSPA. Lastly, while it may come as a surprise to some, the reliability of the MPM-T assembly is expected to be on par with, if not better than, that of an SSPA. The output power of some sample MPMs and MMPMs is shown in Figure 7.

Future directions in power module development point to the continued evolution of microwave power module performance and functionality.

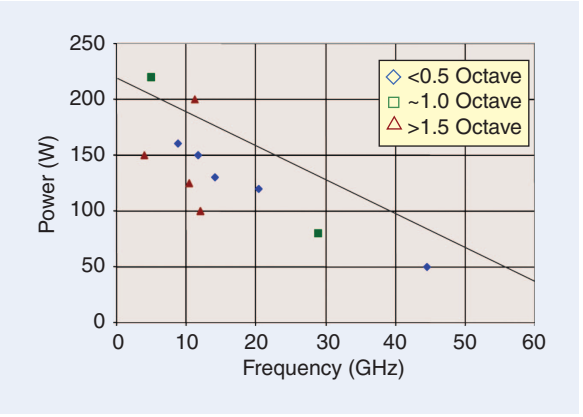

Figure 7. *Average output power of sample microwave power modules (MPMs). The diamonds are MPMs with less than 0.5 octave bandwidth; the squares are MPMs with one octave bandwith; the triangles are MPMs with greater than 1.5 octave bandwidth.*

Current Status of Klystron Amplifiers

Klystrons operate from UHF to millimeter-wave frequencies. They possess high gain, dynamic range, power, efficiency, and low noise, albeit with relatively narrower bandwidths compared to TWTAs. Among the many applications for klystrons is their long use as the workhorse for high-power transmitters in terrestrial broadcast and satellite communications. Continued technical improvements have further reaffirmed their dominance. In [31], by incorporating MSDC, the saturation efficiency for a 2.4 kW klystron designed for direct broadcast satellite (DBS) band was raised from 24% to 40%. This improvement can result in savings of over US$10,000 in energy costs per year. This MSDC technology has led Communications & Power Industries's (CPI's) GEN IV klystron to capture 95% of the satellite communications uplink klystron power amplifier (KPA) market [32]. The typical available power for commercial satellite communications klystron amplifiers is also shown in Figure 5.

For many applications, a klystron is constrained by high voltage, limited bandwidth, and declining power at high frequency. Two noteworthy technologies have been developed to address these issues: the extended-interaction klystron (EIK) and the multiple-beam klystron (MBK).

In the EIK, one or more of the klystron cavities are replaced by structures containing more than one interaction gap. Compared to conventional klystrons, EIKs have a wider bandwidth and a higher power level because of the distributed interaction. The most interesting development in the EIK has been at the millimeter-wave frequencies [33]. EIKs are available at frequencies from Ka-band to G-band. For example, an EIK is capable of delivering an average power of 400 W at 95 GHz and 9 W (CW) at 218 GHz [34].

MBKs offer the advantages of reduced beam voltage, reduced size and weight, and increased bandwidth when compared with single-beam klystrons. Multiple-beam devices have been developed extensively in Russia [35]. The highest level in compactness may well have been achieved by ISTOK (Russia), which developed a Ku-band MBK capable of delivering 0.4 kW of peak power (133 W average) weighing only 400 g, including the magnet.

Advances in Wideband TWTA Linearization

During the past five years, there has been great progress in the linearization of TWTAs. Linearization is still primarily by means of predistortion because of the wider bandwidth and higher efficiencies achievable by this form of linearization. Both analog and digital (digital-signal-processing based) linearization are now being applied to TWTAs. Digital linearization offers the advantage of near ideal transfer response correction. A two-tone carrier-to-intermodulation ratio of greater than 50 dB can be achieved with a TWTA at 3 dB output power backoff from saturation.

The major constraint of digital-based linearization is bandwidth. Although it is now possible to digitally process signals over greater than 1 GHz of bandwidth,

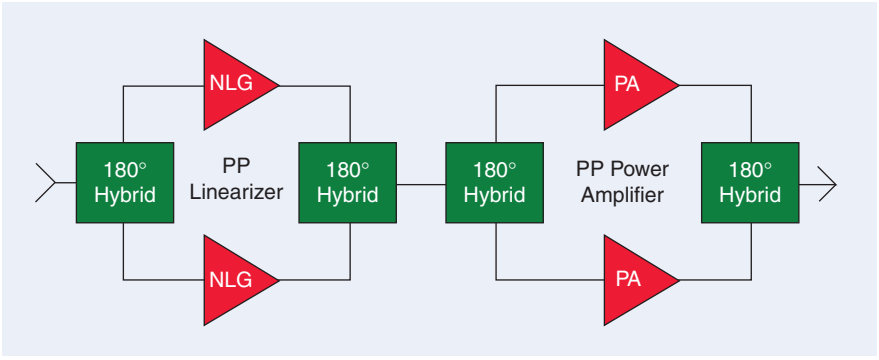

Figure 8. *A push-pull (PP) configuration may be used to minimize both linearizer and traveling-wave tube amplifier even order distortion. NLG: nonlinear generator.*

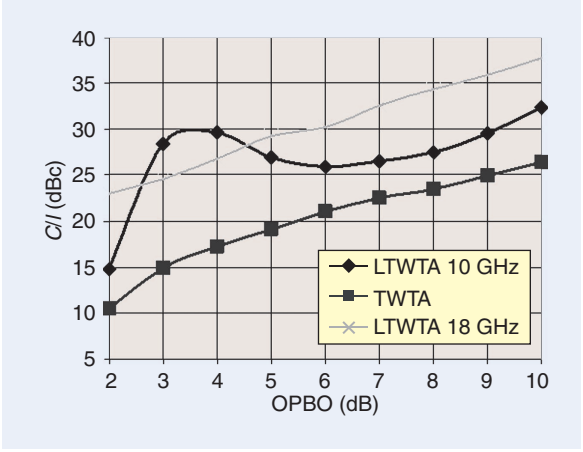

Figure 9. *Wideband linearized traveling-wave tube amplifier (LTWTA) performance. Carrier-to-intermodulation (C/I) ratio versus output power backoff (OPBO) from saturation.*

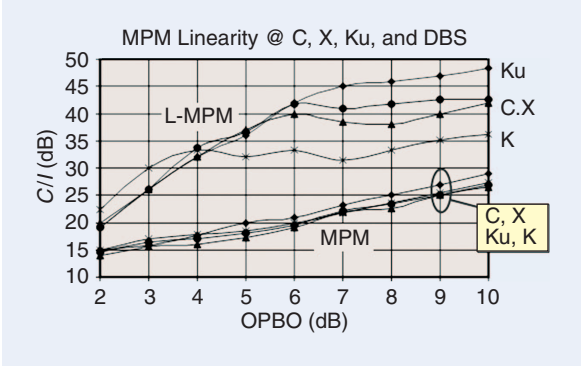

Figure 10. *Carrier-to-intermodulation (C/I) ratio of a quad band linearized microwave power module (L-MMPM) versus output power backoff (OPBO) from saturation.*

practical bandwidths are presently 100 MHz or less due to limitations relating to the complexity, cost, and power consumption of available digital components.

There has been significant progress in extending the bandwidth of analog linearization. It was not very long ago that a 20% bandwidth was considered wideband. Today, multioctave, multi-GHz bandwidths have been achieved [36]. For amplifiers of an octave or greater bandwidth, both even- and odd-order distortion products and both intermodulation and harmonic distortion are present. A linearizer must correct both to achieve linear performance. Even order distortion can be minimized by the use of a push-pull structure. One approach is to use push-pull TWTs to minimize amplifier even-order distortion. Since the nonlinear generators used in the linearizer to correct odd-order intermodulation distortion also produce some even-order distortion that can contribute to overall power amplifier distortion, a push-pull linearizer architecture must also be used. This design approach is illustrated in Figure 8, which shows both a push-pull linearizer and the push-pull PA. If more suppression is required, an even-order nonlinear generator can be used to supplement the odd-order nonlinearity. Figure 9 shows measured LTWTA data taken over a 10–18 GHz range.

In many wideband high-power amplifier applications, performance is not required across the full frequency range but only at specific bands. For such applications, multiband linearizers may provide better performance than a single wideband linearizer. Dual- and triband linearizers have been developed and are in production for C-, X-, and Ku-band. This approach uses two or three independent predistortor modules that can be switched between common input and output amplifiers and attenuators. Using this approach, each predistorter can be aligned for optimum performance in a particular frequency band. The carrier-to-intermodulation ratio performance achieved by an experimental quad-band LTWTA is shown in Figure 10.

In general, with TWTAs, the narrower the bandwidth, the higher the improvement that can be obtained by linearization, but substantial improvement over large continuous bandwidths of more than an octave can be achieved.

Future Trends in Vacuum Electronics Research

New applications, such as high-data-rate communication, high-resolution radar, and active imaging in the millimeter-wave and submillimeter-wave bands, demand the availability of compact higher-power sources at these frequencies and will be the driving force for vacuum electronics research in the near future. The two current Defense Advanced Research Projects Agency (DARPA) programs developing amplifier technologies at these frequencies are HiFIVE and Terahertz

Electronics. HiFIVE is developing amplifiers at 220 GHz, and Terahertz Electronics is developing them at 670, 850, and 1030 GHz. They both include vacuum electronics technologies. The emerging requirements will continue to push the vacuum electronics field to new levels of performance through advances in areas such as new physics-based advanced modeling and simulation tools, innovative cathodes, and new fabrication techniques. Spatially distributed electron beams such as multiple beams and sheet-beam topologies supported by microfabrication and refinements in materials, magnetics, and electron sources, will contribute to growth opportunities. Advances in power supply technology may well be an important next step in size reduction. Examples of these research efforts are given in the following sections.

Cold Cathodes for Vacuum Electronics Amplifiers

The cathode lies at the heart of every vacuum electronics RF amplifier, powering the energy-exchange circuitry for conversion of electron kinetic energy to energy of a propagating electromagnetic wave. The cathode's sole purpose is to create a high-energy electron beam that streams through the vacuum in relative proximity to the device's RF circuit. Current technology employs almost exclusively thermionic cathodes—i.e., metallic composites that are heated by various means to near 1,000 °C. At such temperatures, electrons that are normally bound to the cathode's metallic lattice can be extracted from the cathode surface if their thermal energies exceed the cathode's surface vacuum potential barrier. This method of creating free-streaming electron beams in a vacuum has been successively employed for more than 60 years.

Quantum mechanics, however, holds the promise of fundamentally altering the method used to create streaming electron beams in vacuums—one that will enable revolutionary performance gains for the devices that employ it. These cold cathodes do not require high thermal electron energies for beam emission, but instead rely on quantum mechanical tunneling though the vacuum potential barrier, a barrier distorted by the creation of high cathode surface electric fields. Figure 11 depicts the potential energy diagram for electrons at the surfaces of a thermionic cathode and a cold cathode, both at room temperature. In the case of the thermionic cathode, without additional energy $q_e \Delta\varphi$, the electrons are bound to the cathode surface and cannot escape into the vacuum. The additional energy required must come from direct heating of the cathode via external means.

In the case of the cold cathode, no additional thermal energy is available. Instead, the shape of the vacuum barrier is distorted via application of a high electric field to the cathode surface. The barrier is not reduced to zero, however, and the cathode relies on quantum mechanical tunneling through the barrier, which allows for transit of electrons through

Multiple-beam klystrons offer the advantages of reduced beam voltage, reduced size and weight, and increased bandwidth.

the forbidden zone with a nonzero probability. If the surface electric field and vacuum barrier distortion become high enough, then the tunneling probability increases to levels that allow sufficient vacuum current to be extracted.

To create the necessary high cathode surface fields, new methods of cathode fabrication have been developed that replace the metal composites of the thermionic cathode with a microfabricated silicon substrate upon which are formed several electric field-enhancing features. Figure 12 compares the surface geometry and electric field values of (a) a thermionic cathode, (b) a microfabricated cold cathode substructure with field-enhancing dielectric layer, and (c) a microfabricated cold cathode with a field-enhancing dielectric layer and an additional field-enhancing cone emitter. The dielectric layer increases the electric field over that of a thermionic cathode by about 100 times, and the cone emitters add an additional factor of 10–100 times at the apex of the cone, creating electric fields that ultimately exceed the threshold for room temperature electron emission into the vacuum.

The cone emitters of Figure 12(c) have micron-sized features, and, typically, each produce 1–10 mA of vacuum current. The small feature size and use of microfabrication techniques allow for large arrays of such emitters $(10^4 - 10^5)$ to be manufactured onto

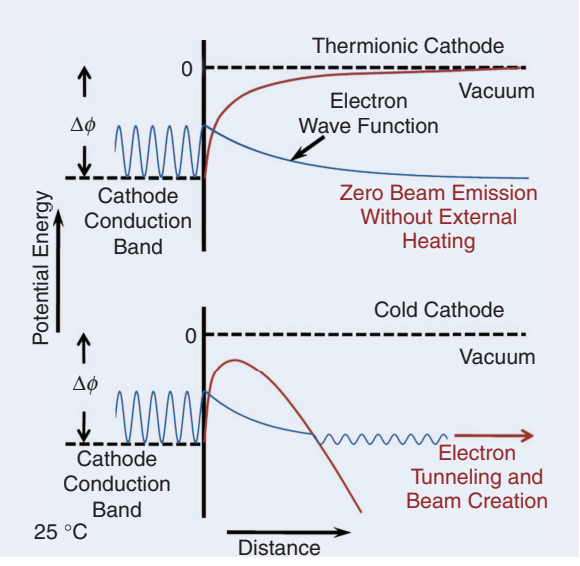

Figure 11. *Energy diagram for a thermionic cathode and a cold cathode. The high surface electric field for the cold cathode distorts the potential barrier and allows tunneling.*

If vacuum electronics amplifiers can be developed to fully exploit the capabilities of the cold cathode, new vistas of operating performance can be realized.

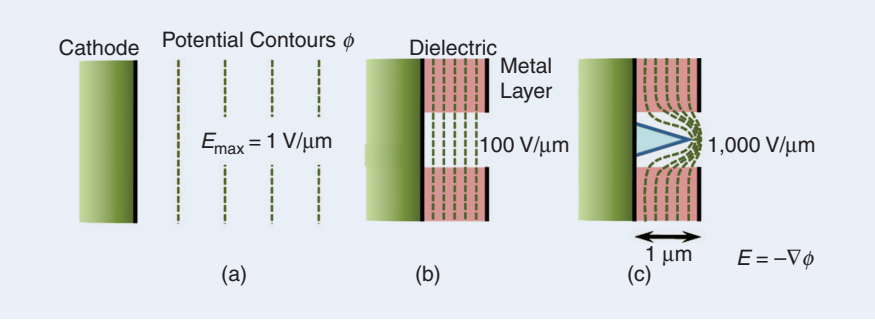

Figure 12. *Cathode surface geometry of (a) thermionic cathode, (b) microfabricated cold cathode substructure with field-enhancing dielectric layer, and (c) microfabricated cold cathode with dielectric layer and additional field-enhancing cone emitter.*

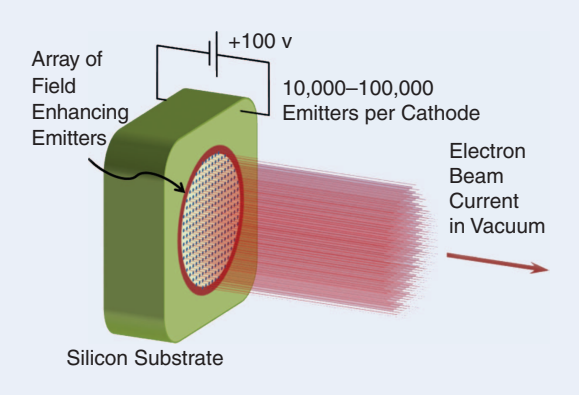

Figure 13. *An embodiment of a cold cathode array.*

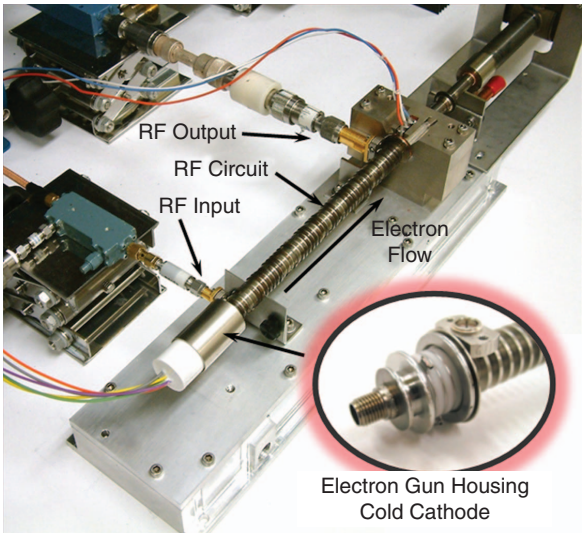

Figure 14. *Photograph of a 100 W cold cathode traveling-wave tube.*

very small cathode substrates, typically more than an order of magnitude smaller than a thermionic cathode producing the same total current. Figure 13 shows a typical embodiment of a cold cathode array. Unlike a thermionic cathode, the cathode structure is relatively simple. Application of about 100 V across the cathode substrate is sufficient to extract a full-current beam. This simple implementation eliminates the entire cathode heating structure and support necessary for the operation of its thermionic counterpart.

Development of microwave devices that employ cold cathodes of the type shown in Figures 12 and 13 have been ongoing for the past 15 years [37]–[41], with performance levels steadily increasing over this period. In the past year, performance approaching levels required for use in actual microwave systems has been achieved in a cold cathode TWT developed at L-3 Communications Electron Devices in San Carlos, California [42], with cathodes developed at SRI International in Menlo Park, California [43]. Figure 14 shows a photograph of the device, including the cold cathode electron gun and the RF amplification circuit.

The RF power and efficiency performance of the cold cathode TWT is shown in Figure 15 for values of current ranging from zero to the device's full operating value. The TWT demonstrates operation at 100 W and 5 GHz, 22 dB saturated gain, 33 dB small signal gain, beam currents up to 0.120 A, and duty factors up to 10%. These operating parameters are relevant for some existing communication, data link, and radar applications.

If vacuum electronics amplifiers, such as those shown in Figures 14 and 15, can be developed to fully exploit the capabilities of the cold cathode, new vistas of operating performance can be realized. The cold cathode has the potential to affect all aspects of operation, including maximum device frequency, lifetime and reliability, fast turn-on time, maximum modulation rate, size, linearity, and efficiency. Given their miniature size, cold cathodes make high current density operation possible without the inherent life-limiting mechanism encountered with thermionic devices; this characteristic becomes increasingly important as compact high-frequency sources are further developed in coming years. Operation at room temperature eliminates the complex electron gun design and cathode manufacturing technologies required to heat the cathode to near the required 1,000 °C while limiting the temperature rise and differential thermal expansion

of surrounding gun material. Instant device turn-on is also possible with devices employing cold cathodes. Time scales for cold cathode turn-on from an off state to fully on state are decreased by several orders of magnitude, as the thermionic cathode responds on thermal diffusion time scales of seconds, while the cold cathode responds on voltage charging time scales of tens of nanoseconds. In addition, the turn-on voltage for these cathodes is reduced by an order of magnitude below that of an electrode-modulated thermionic cathode, thereby reducing modulator voltage requirements and increasing modulation rates, both by an order of magnitude. The importance of and benefit derived from cold cathode implementation depends on the intended application, though the potential of this newly developed technology to affect the ultimate performance limits of all RF vacuum devices is clear.

Sheet-Beam Amplifiers

Sheet-beam millimeter-wave amplifiers offer the prospect of considerably higher power and specific power (output power per unit weight and volume) than can be achieved with comparable pencil-beam devices because significantly higher current can be transported through the circuit at a given voltage. This advantage is particularly important as the frequency of vacuum electronics amplifiers increases to 100 GHz and beyond because the dimensions of the beam tunnel, as well as the slow-wave structure, scale as the wavelength λ. In a pencil-beam device, the beam diameter must be approximately $\lambda/10$ or less. Space-charge forces and beam temperature effects fundamentally limit the current that can be transported in such a small diameter beam thus limiting the power that can be generated. The power density of the electromagnetic field that can be supported by the beam-wave interaction structures and couplers is also limited by breakdown and heating effects, imposing an additional limitation on the output power as the volume of these structures decreases with increasing frequency. Empirically, the output power scales roughly as λ^3. To overcome these limitations while retaining the many positive features of slow-wave or standing-wave amplifiers, it is necessary to somehow increase the beam cross-section and the beam-wave interaction volume. Sheet beams provide a solution. An example sheet structure is shown in Figure 16.

Sheet-beam devices are also attractive because the planar topology is relatively simple to fabricate. This is particularly important at millimeter-wave and terahertz frequencies, where the very small feature sizes and tolerances can be achieved by lithographic microfabrication techniques, such as lithography, electroplating, and molding and deep reactive-ion etching. However, the successful development and implementation of sheet-beam devices also present some difficult challenges that have so far severely limited

Sheet-beam millimeter-wave amplifiers offer the prospect of considerably higher power than can be achieved with comparable pencil-beam devices.

the realization of this technology. In fact, sheet beam amplifiers have been pursued for well over 50 years [44], but, generally, they have yet to be proven as a practical alternative to pencil-beam devices. There are a number of reasons for this arrested development. First and perhaps the most fundamental is that the basic advantage of a sheet beam only holds if the electron current density can be maintained at approximately the same level of the corresponding pencil beam, and this is quite difficult due to potential sheet beam instabilities, edge effects, and nonuniformities. A high degree of uniformity of both the beam and the RF field across the width of the sheet is necessary

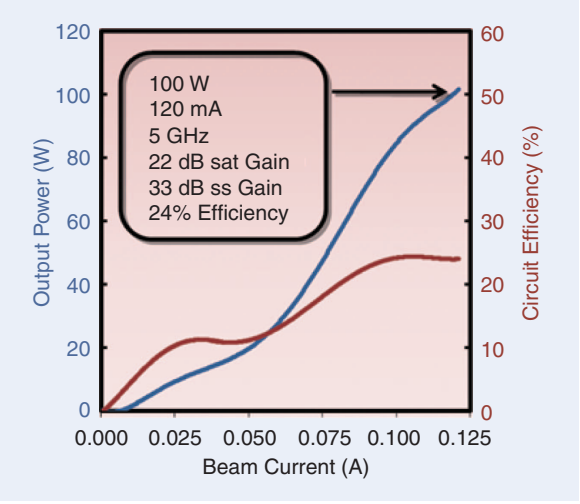

Figure 15. *Measured cold cathode traveling-wave tube power and efficiency performance data.*

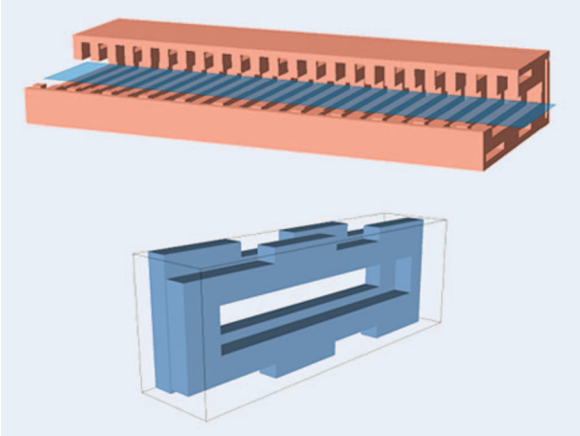

Figure 16. *Sheet beam coupled-cavity traveling wave structure with expanded view of one cell.*

for strong and efficient beam-wave interaction. Also, sheet-beam interaction circuits are intrinsically overmoded, and fabrication errors or slight misalignments of the beam relative to the circuit can cause undesired modes to be excited. Thus, two major obstacles that must be overcome to achieve the full potential of sheet-beam amplifiers are 1) the formation and transport of a sufficiently high perveance and uniform beam and 2) the design and fabrication of suitable interaction circuits, both of which must be executed with a high degree of precision.

Most sheet beam research has focused on magnetic transport, utilizing periodic permanent magnets [45], [46]. Such a configuration is relatively light and compact, and stable beam transport can be achieved over a relatively long length. The key disadvantage of periodic permanent magnet focusing is that it imposes a minimum beam voltage for stability that is often far higher than desirable from systems considerations. The alternative magnetic focusing scheme, employing a uniform or solenoidal field, can provide significantly higher field strength (and hence stronger focusing) from available permanent magnets than periodic permanent magnet focusing, but it has usually been avoided because of potential instabilities [47].

To determine the optimum transport technique for a sheet beam, these stability considerations must be combined with the beam envelope equation, which determines the magnetic field strength required to balance the outward space-charge and beam temperature forces on the beam. For relatively low-voltage (<20–25 kV) sheet beam devices, a solenoidal field can transport significantly higher current densities, thereby achieving higher output power [48]. The price that must be paid is a somewhat heavier and larger magnet assembly. Whichever approach is used, the transport field must be carefully matched to the electron gun.

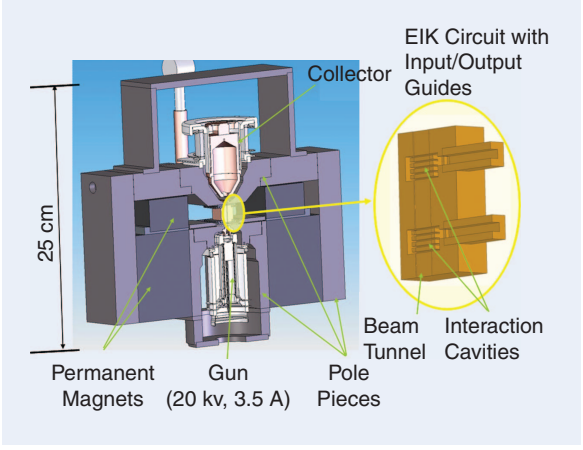

Figure 17. *Layout of NRL's 94 GHz sheet-beam extended interation klystron (EIK). The permanent magnet produces a uniform 8.5-kG field over the interaction volume.*

Most sheet-beam circuit configurations that have been considered for millimeter-wave amplifiers are either like EIK, consisting of a number of discrete cavity structures, or traveling-wave types, with a suitable structure to slow the wave phase velocity to match the electron velocity. While these configurations are generally analogous to corresponding well-developed pencil-beam structures, their design and optimization are complicated and quite challenging. Unlike the beam tunnel in pencil-beam devices, which is below cut-off for the operating frequency so that adjacent circuit elements are isolated, a sheet beam tunnel is wide enough to propagate the fundamental transverse electric (TE) mode, which can easily be excited and lead to oscillation and/or beam disruption if the midplane symmetry of the tunnel, circuit, and beam is destroyed by misalignment, fabrication errors, etc. Also, as the aspect ratio of a sheet beam device increases, it becomes more difficult to ensure uniformity and proper phasing of the beam and the mode field across the entire width of the device.

Recent progress in devising such sheet beam structures, largely facilitated by more powerful computer codes and computing resources, is promising. These codes are enabling much more realistic designs to be evaluated and, with their optimization routines to fine-tune parameters, make first-pass fabrication success a reality. As an example, such simulations predict that a 94-GHz, 20-kV, 3.5-A sheet-beam EIK, which has an interaction circuit <1.5 cm long, can generate a peak output power >10 kW. This is at least a factor of five larger than a pencil-beam device at this frequency and operating voltage. A device based on this simulation is being fabricated (Figure 17), and efforts are underway to scale such devices into the terahertz regime.

Compact, High-Power Terahertz Sources

Since demonstrating the first operation of a vacuum electronic terahertz source based on microfabricated folded-waveguide (FWG) technology [49], Northrop Grumman has continued the development of compact, high-power THz sources in support of several DARPA THz initiatives. Similar to classical vacuum electronic devices, these THz sources consist of a thermionic electron source, a slow-wave interaction circuit to amplify the RF wave, and a depressed collector to recover energy from the spent beam for efficient source operation. A 10 kG Nd-Fe-B permanent magnet solenoid is used to magnetically confine the electron beam as it passes through the slow-wave structure. Vacuum electronics devices based on FWG regenerative oscillator circuits have been successfully fabricated and operated between 0.600–0.675 THz with RF power levels over 50 mW at duty cycles up to 3% [50]. This is significantly higher than the power capability of existing sources operating at these frequencies.

A FWG slow-wave circuit is a serpentine waveguide, folded back upon itself multiple times, with a beam tunnel through the center of the structure. The FWG is designed such that the axial velocity of the RF wave in the waveguide can be made to match the group velocity of the electrons travelling down the beam tunnel. In order to achieve efficient coupling of the RF wave to the electron beam at THz frequencies, the cross-sectional dimensions of the FWG are on the order of tens of microns by hundreds of microns, which must not vary over the entire circuit length of several centimeters.

Another requirement is smooth walls to minimize the waveguide attenuation due to the shallow skin depth at THz frequencies. Realization of circuits meeting these requirements has only been enabled by the use of modern microfabrication techniques, like deep reactive-ion etching of silicon coupled with copper sputter deposition and electroplating. The planar nature of the FWG circuit is naturally amenable to these planar microfabrication processes, enabling batch processing of multiple circuits on a single wafer. Additionally, FWG circuits do not rely on fragile structures such as gratings to achieve amplification, and, therefore, they are structurally more robust. They are fabricated from a solid block for better thermal management. Finally, cofabricated tapers at each end of the serpentine waveguide provide a natural and effective way for coupling power into and out of the circuit. The FWGs used in the terahertz sources (Figure 18) were fabricated in halves (mirror-images) by a two-level silicon deep reactive-ion etching process: One step to create the FWG itself and a second step to create the beam tunnel through the FWG structure. Each half was then metalized via copper electroplating, aligned, and bonded together, forming the completed FWG circuit.

In addition to the careful design and accurate fabrication of the FWG interaction circuit, the electrostatic gun design, electron beam transport magnetics, and the collector design are crucial in order to achieve compact, high-power devices that operate with minimal beam intercept and high device efficiency. Focus and transport of a 4 mA beam through the $60 \times 60\ \mu m^2$ beam tunnel ($60\ \mu m$—roughly the diameter of an average human hair) is a technical challenge as mechanical offsets, edge-emitted electrons from the cathode, and localized transverse magnetic fields on the order of a few tens of Gauss (less than 1% of the overall axial field) can force the beam off axis, leading to significant beam intercept. Precision fabrication of the electron gun assembly, accurate mechanical alignment of the gun with the beam tunnel in the FWG circuit, and minimization of the transverse magnetic fields have lead to a beam transmission of 78% for a 4.8 mA beam at 10 kV in a recent prototype. Lastly, the design of a single-stage, graphite lens collector was optimized to recover 92.4% of the energy from the spent electron beam. The THz source prior to final assembly is shown in Figure 19.

After assembly and exhaust, the vacuum electronics FWG THz source is mounted on the test stand in the bore of the permanent magnet solenoid. Beam focus and transmission are controlled by the alignment of the magnet, which is adjusted, relative to the source, with two three-axis translation stages. A cylindrical copper waveguide serves as an overmoded, external output waveguide to transmit RF output power to

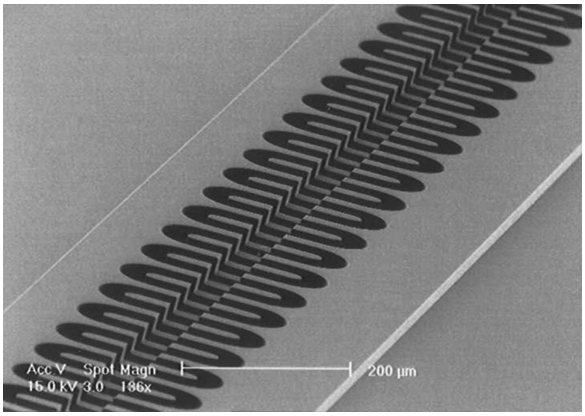

Figure 18. *Folded-waveguide circuit half fabricated by deep reactive-ion etching process.*

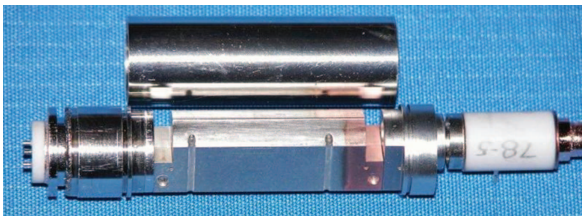

Figure 19. *The terahertz source prior to final assembly.*

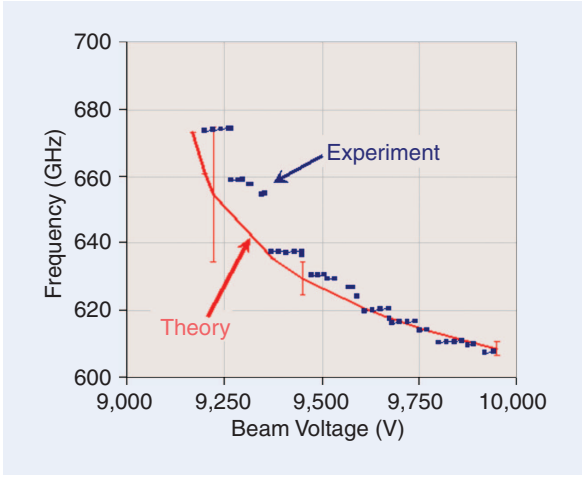

Figure 20. *Terahertz source operating frequencies.*

At millimeter-wave bands, the performance of vacuum electronics devices is not likely to be matched by solid-state power amplifiers in the near future.

the THz detector. A 2 L/s ion pump maintains the vacuum, and nitrogen gas flows through the magnet bore to stabilize the temperature of the source during testing.

Table 1 summarizes the operating characteristics for a recent THz source prototype. This source operated at 0.656 THz, 9.9 kV, and 46% beam transmission. Measured power at the output window was 52 mW. In the oscillator, the estimated single pass gain is around 15 dB, which is equal to the total loss of the return path. The size of the compact device is driven mainly by the size of the cylindrical magnet with a diameter of 3.4 in and a length of 4.9 in.

The oscillation frequency is observed to step-tune as the beam voltage is varied from 9.6 kV to greater than 10 kV, as shown in Figure 20. It is believed that these steps are characteristic of the regenerative feedback FWG circuit in the source. In general, there was megahertz stability from pulse to pulse. The measured line-width was less than 30 MHz due, in part, to fluctuations of the beam current and voltage during the pulse. Measurable power was observed between 607–675 GHz.

Work is presently underway to extend FWG device technology to develop compact, high-power vacuum electronic amplifiers and fully integrated power modules (a solid-state driver amplifier together with a FWG amplifier) to operate from 0.2 THz to over 1 THz.

TABLE 1. THz source operation parameters.

Parameter	Value
Power at window	52 mW
Frequency	0.656 THz
Single pass gain	~15 dB
Cathode voltage	9.9 kV
Pulse length	0.05–1.0 ms
Repetition rate	≤30 Hz
Duty cycle, maximum	3 %
Axial field	10 kG
Emission current	4.6 mA
Collector current	2.1 mA
Beam transmission	46 %
Interaction efficiency	0.4 %
Source efficiency	0.2 %

Conclusion

Vacuum electronics amplifiers continue to play an important role in high-power transmitter applications. At microwave frequencies, recent advances in wide bandgap semiconductor devices such as GaN and power combining techniques are enabling SSPAs to challenge the power advantage of vacuum electronics amplifiers, but vacuum electronics devices still hold the efficiency edge even at these frequencies. At millimeter-wave bands, the performance of vacuum electronics devices, both in terms of power bandwidth product and efficiency, is not likely to be matched by SSPAs in the near future. The use of linearization further enhances the efficiency edge of vacuum electronics amplifiers. The development of technology at the upper millimeter-wave and submillimeter-wave are enabled by cold cathode technologies and microfabrication techniques.

References

[1] A. S. Gilmour, Jr., *Principles of Traveling Wave Tubes*. Boston: Artech House, 1994.

[2] A. S. Gilmour, Jr., *Microwave Tubes*. Boston: Artech House, 1986.

[3] R. J. Barker, J. H. Booske, N. C. Luhmann, Jr., and G. S. Nusinovich, Eds., *Modern Microwave and Millimeter-Wave Power Electronics*. Piscataway, NJ: IEEE Press, 2005.

[4] V. S. Bajaj, M. K. Hornstein, K. E. Kreischer, J. R. Sirigiri, P. P. Woskov, M. L. Mak-Jurkauskas, J. Herzfeld, R. J. Temkin, and R. G. Griffin, "250 GHz CW gyrotron oscillator for dynamic nuclear polarization in biological solid state NMR," *J. Magn. Reson.*, vol. 189, no. 2, pp. 251–279, Dec. 2007.

[5] R. K. Parker, R. H. Abrams, Jr., B. G. Danly, and B. Levush, "Vacuum electronics," *IEEE Trans. Microw. Theory Tech.*, vol. 50, no. 3, pp. 835–845, Mar. 2002.

[6] R. H. Abrams, Jr., B. Levush, A. A. Mondelli, and R. K. Parker, "Vacuum electronics for the 21st century," *IEEE Microw. Mag.*, vol. 2, no. 3, pp. 61–72, Sept. 2001.

[7] A. V. Galdetskiy, "Helix slow-wave structure with diamond support for power TWTs," in *Proc. 6th Int. Vacuum Electronics Conf.*, Noordwijk, The Netherlands, Apr. 2005, pp. 471–472.

[8] J. M. Weekley and B. J. Mangus, "TWTA versus SSPA: A comparison of on-orbit reliability data," *IEEE Trans. Electron Devices*, vol. 52, no. 5, pp. 650–652, May 2005.

[9] "Solid-state power invades the tube realm," in *Proc. IEEE MTT-S Int. Microwave Symp. Workshop*, Honolulu, HI, June 2007.

[10] H. Shigematsu, Y. Inoue, A. Akasegawa, M. Yamada, S. Masuda, Y. Kamada, A. Yamada, M. Kanamura, T. Ohki, K. Makiyama, N. Okamoto, K. Imanishi, T. Kikkawa, K. Joshin, and N. Hara, "C-band 340-W and X-band 100-W GaN power amplifiers with over 50-% PAE," in *Proc. Int. Microwave Symp.*, Boston, MA, June 2009, TH3A-1.

[11] H. Sumi, H. Takahashi, T. Soejima, and R. Mochizuki, "Ku-band, 120-W power amplifier using gallium nitride FETs," in *IEEE MTT-S Int. Microwave Symp. Dig.*, Boston, MA, June 2009, *TH4A-3*.

[12] "Millimeter-wave power amplifier technology: Power, linearity and efficiency," in *Proc. IEEE MTT-S Int. Microwave Symp. Workshop*, Atlanta, GA, June 2008.

[13] General Dynamics SATCOM Technologies. [Online]. Available: http://www.gdsatcom.com/electronics.php#solid

[14] M. Cascone, *CPI, private communication,* Sept. 2006.

[15] W. L. Menninger, S. T. Blunk, and W. L. McGeary, "Seventy percent efficient flight set average Ku-band traveling wave tubes for satellite communications," in *Proc. 7th Int. Vacuum Electronics Conf.*, Monterey, CA, Apr. 2006, pp. 21–22.

[16] S. Van Fleteren. *Traveling wave tube vs. solid state amplifiers* [Online]. Available: http://www.djmelectronics.com/articles/twt-vs-solid-state.html

[17] A. Katz, "Linearization: Reducing distortion in power amplifiers," *IEEE Microw. Mag.*, vol. 2, no. 4, pp. 37–49, Dec. 2001.

[18] J. X. Qiu, D. K. Abe, T. M. Antonsen, Jr., B. G. Danly, B. Levush, and R. E. Myers, "Linearizability of TWTAs using predistortion techniques," *IEEE Trans. Electron Devices*, vol. 52, no. 5, pp. 718–727, May 2005.

[19] D. M. Goebel, R. R. Liou, W. L. Menninger, X. Zhai, and E. A. Adler, "Development of linear traveling wave tubes for telecommunications applications," *IEEE Trans. Electron Devices*, vol. 48, no. 1, pp. 74–81, Jan. 2001.

[20] D. Chernin, T. M. Antonsen, Jr., B. Levush, S. J. Cooke, and W. Manheimer, "A comparison of linearity and efficiency in conventional and transverse TWT amplifiers," *IEEE Trans. Electron Devices*, vol. 54, no. 2, pp. 194–201, Feb. 2007.

[21] A. Laurent, M. Lefevre, T. Barsotti, D. Chesnel, A. Brechenmacher, and P. Thouvenin, "High-power C- and X-band radar helix TWTs," *IEEE Trans. Electron Devices*, vol. 56, no. 5, pp. 906–912, May 2009.

[22] C. K. Chong, J. A. Davis, R. H. Le Borgne, M. L. Ramay, R. J. Stoltz, R. N. Tamashiro, J. P. Vaszari, and X. Zhai, "Development of high-power Ka-band and Q-band helix TWTs," *IEEE Trans. Electron Devices*, vol. 52, no. 5, pp. 653–659, May 2005.

[23] J. Petillo, K. Eppley, D. Panagos, P. Blanchard, E. Nelson, N. Dionne, J. DeFord, B. Held, L. Chernyakova, W. Krueger, S. Humphries, T. McClure, A. Mondelli, J. Burdette, M. Cattelino, R. True, K. T. Nguyen, and B. Levush, "The MICHELLE three-dimensional electron gun and collector modeling tool: Theory and design," *IEEE Trans. Plasma Sci.*, vol. 30, no. 3, pp. 1238–1264, June 2002.

[24] D. Chernin, T. M. Antonsen, Jr., B. Levush, and D. R. Whaley, "A three-dimensional multifrequency large signal model for helix traveling wave tubes," *IEEE Trans. Electron Devices*, vol. 48, no. 1, pp. 3–11, Jan. 2001.

[25] S. J. Cooke, C.-L. Chang, T. M. Antonsen, Jr., D. P. Chernin, and B. Levush, "Three-dimensional modeling of AC space charge for large-signal TWT simulation," *IEEE Trans. Electron Devices*, vol. 52, no. 5, pp. 764–773, May 2005.

[26] CPI company Web site. [Online]. Available: http://www.cpii.com/product.cfm

[27] C. Smith, C. M. Armstrong, and J. Duthie, "The microwave power module: A versatile RF building block for high-power transmitters," *Proc. IEEE*, vol. 87, no. 5, pp. 717–737, Mar. 1999.

[28] MPM tutorial [Online]. Available: http://www.l-3com.com/edd/mpm/mpm_flash.htm

[29] R. S. Symons, "Modern microwave power sources," *IEEE Aerosp. Electron. Syst. Mag.*, vol. 17, no. 1, pp. 19–26, Jan. 2002.

[30] A. Katz and R. Gray, "The linearized microwave power module," in *IEEE MTT-S Int. Microwave Symp. Dig.*, June 2003, pp. 335–338.

[31] E. L. Wright, R. Batra, R. Begum, E. McCune, A. Shabazian, and L. Zitelli, "Multistage depressed collector klystron development and production," in *Proc. 2nd Int. Vacuum Electronics Conf.*, Noordwijk, The Netherlands, Apr. 2001, pp. 111–112.

[32] M. Cascone, *CPI, private communication,* Jan. 2005.

[33] A. Roitman, P. Horoyski, M. Hyttinen, D. Berry, and B. Steer, "Extended interaction klystrons for submillimeter applications," in *Proc. 7th Int. Vacuum Electronics Conf.*, Monterey, CA, Apr. 2006, p. 191.

[34] M. Hyttinen, A. Roitman, P. Horoyski, R. Dobbs, E. Sokol, D. Berry, and B. Steer, "A compact, high power, sub-millimeter-wave extended interaction klystron," in *Proc. 9th Int. Vacuum Electronics Conf.*, Monterey, CA, Apr. 2008, p. 297.

[35] A. N. Korolyov, E. A. Gelvich, Y. V. Zhary, A. D. Zakurdayev, and V. I. Poognin, "Multiple beam klystron amplifiers: Performance parameters and development trends," *IEEE Trans. Plasma Sci.*, vol. 32, pp. 1109–1118, June 2004.

[36] A. Katz, R. Gray, and R. Dorval, "Wide/multiband linearization of TWTAs using predistortion," *IEEE Trans. Electron Devices*, vol. 56, no. 5, pp. 959–964, May 2009.

[37] M. Garven, S. N. Spark, A. W. Cross, S. J. Cooke, and A. D. R. Phelps, "Gyrotron experiments employing a field emission array cathode," *Phys. Rev. Lett.*, vol. 77, no. 11, pp. 2320–2323, Sept. 1996.

[38] S. G. Bandy, M. C. Green, C. A. Spindt, M. A. Hollis, W. D. Palmer, B. Goplen, and E. G. Wintucky, "Application of gated field emitter arrays in microwave amplifier tubes," in *Proc. IEEE Int. Vacuum Microelectronics Conf.*, Ashville, NC, 1998, p. 132.

[39] H. Makishima, S. Miyano, H. Imura, J. Matsuoka, H. Takemura, and A. Okamoto, "Design and performance of traveling wave tubes using field emitter array cathodes," *Appl. Surf. Sci.*, vol. 146, pp. 230–233, Nov. 1999.

[40] D. R. Whaley, B. Gannon, C. Smith, C. M. Armstrong, and C. A. Spindt, "Application of field emitter arrays to microwave power amplifiers," *IEEE Trans. Plasma Sci.*, vol. 28, no. 3, pp. 727–747, June 2000.

[41] D. R. Whaley, B. Gannon, V. O. Heinen, K. E. Kreischer, C. E. Holland, and C. A. Spindt, "Experimental demonstration of an emission-gated traveling wave tube amplifier," *IEEE Trans. Plasma Sci.*, vol. 30, no. 3, pp. 998–1008, June 2002.

[42] D. R. Whaley, R. Duggal, C. M. Armstrong, C. L. Bellew, C. E. Holland, and C. A. Spindt, "100 Watt operation of a cold cathode TWT," *IEEE Trans. Electron Devices*, vol. 56, no. 5, pp. 896–905, May 2009.

[43] P. R. Schwoebel, C. A. Spindt, and C. E. Holland, "Spindt cathode tip processing to enhance emission stability and high-current performance," *J. Vac. Sci. Technol. B*, vol. 21, no. 1, pp. 433–435, Jan. 2003.

[44] O. Buneman, "Ribbon beams," *Int. J. Electron.*, vol. 3, no. 5, pp. 507–509, May 1957.

[45] B. E. Carlsten, S. J. Russell, L. M. Earley, W. B. Haynes, F. Krawczyk, E. Smirnova, Z.-F. Wang, J. M. Potter, P. Ferguson, and S. Humphries, "Mm-wave source development at Los Alamos," in *Proc. 7th Workshop on High Energy Density and High Power RF, AIP Conf. 807*, June 2005, pp. 326–334.

[46] G. Scheitrum, "Design and construction of a W-band sheet beam klystron," in *Proc. 7th Workshop on High Energy Density and High Power RF, AIP Conf. 807*, June 2005, pp. 120–125.

[47] J. H. Booske, B. D. McVey, T. M. Antonsen, Jr., "Stability and confinement of nonrelativistic sheet electron beams with periodic cusped magnetic focusing," *J. Appl. Phys.*, vol. 73, no. 9, pp. 4140–4155, May 1993.

[48] K. T. Nguyen, J. A. Pasour, T. M. Antonsen, Jr., P. B. Larsen, J. J. Petillo, and B. Levush, "Intense sheet electron beam transport in a uniform solenoidal magnetic field," *IEEE Trans. Electron Devices,* vol. 56, no. 5, pp. 744–752, May 2009.

[49] J. Tucek, K. Kreischer, D. Gallagher, R. Vogel, and R. Mihailovich, "Development and operation of a 650 GHz folded waveguide source," in *Proc. 8th Int. Vacuum Electronics Conf.*, Kitakyushu, Japan, May 2007, pp. 219–220.

[50] J. Tucek, K. Kreischer, D. Gallagher, R. Vogel, and R. Mihailovich, "A compact, high power, 0.65 THz source," in *Proc. 9th Int. Vacuum Electronics Conf.*, Monterey, CA, Apr. 2008, pp. 16–17.